ASM Sc. J., 17, 2022

https://doi.org/10.32802/asmscj.2022.1035

Extraction of Silica from Rice Husk Ash and Its Effect on the Properties of the Integral Membrane

N.S.I. Chik, N.Z. Kassim Shaari*, N.A. Ramlee and M.R. Abdul Manaf

School of Chemical Engineering, College of Engineering, Universiti Teknologi MARA, Shah Alam, Selangor, Malaysia

The large generation of agricultural residue could pose an environmental issue that lies through the disposal problem. Therefore, the incorporation of rice husk ash (RHA) into the membrane formulation could curb this problem besides adding value to the biomass. Rice husk ash is widely used as a filler for a polymer composite to enhance its mechanical properties due to the presence of silica. This research incorporated RHA into the membrane formulation. The silica in the RHA was extracted using an acid-leaching process and dried into silica powder. The silica powder was characterised by using an X-Ray diffractometer (XRD) and X-Ray fluorescence (XRF). A sol-gel method with hydrochloric acid as the catalyst was used in the fabrication of polysulfone/chitosan/polyvinyl alcohol membrane, and the extracted silica powder was incorporated in the formulations. The membranes were characterised in terms of functional groups using Fourier Transform Infrared Spectroscopy (FTIR), surface morphology using Scanning Electron Emission (SEM) analysis, and surface hydrophilicity using contact angle analysis. Finally, the performance of the membrane was analysed by pure water flux and antifouling. The XRD and XRF results showed that the extracted silica powder contained 77% of silica with the absence of impurities. The cross-linking reaction of membranes occurred as the Si–O–C bond was detected at 1,105cm^{-1} after the FTIR analysis, and a compact structure of the membrane was detected from the SEM analysis. The results from pure water flux portrayed that the membranes incorporated with silica (M1 and M2) had better integral stability compared to that from the pure polymer, which was observed from the consistent value of flux throughout the 1-hour filtration time and no swelling of the membranes after the performance testing. The results also showed that the extraction of silica from the RHA using a modified process was successfully conducted, and the silica powder was also compatible with the membrane solution as no separate layer was formed. Thus, the produced membranes have the potential to be used in the treatment of wastewater containing heavy metal ions.

Keywords: composite membrane; crosslinking; pure water flux; rice husk ash; silica

I. INTRODUCTION

In previous years, the search for environmentally friendly technology has contributed to the development of some significant areas of interest such as the minimisation of wastes by utilisation of agricultural wastes into the fabrication of polymer composite materials. A paddy, which is one of the most staple food plants, produces rice husk as the by-product that is mostly dumped as a waste, which can create an environmental issue (Setyawan *et al.*, 2019). Only few studies reported the use of this agricultural waste as a filler in a polymer (Jean *et al.*, 2011). Due to its high silica content, rice husk ash (RHA) is widely utilised in ceramic, construction, chemical, and electronic industries in high capacitance activated carbons, photoluminescents, and adsorbents (Edson LF, 2005; You *et al.*, 2019).

The production of silica (SiO_2) within the amorphous state is preferable because it is more active than crystalline silica, as the amorphous silica has higher mechanical properties and higher quality in the non-distractive test than the crystalline

*Corresponding author's e-mail: norinzamiah@uitm.edu.my

silica (Sldozian, 2014). The amorphous form of silica is obtained when the rice husk is burnt between 350 and 750°C, and the crystalline silica form is obtained when burnt over 800°C (Rasoul *et al.*, 2018).

Due to a mild operating temperature, the acid-leaching process is a preferable method for silica extraction from the RHA. The extracted sodium silicate turns into a silica gel after a treatment with acid (HCl). The findings from previous works on the extraction process and characterisation of the silica gel have contributed to the modification of the methods (Samantha *et al.*, 2011). The silica gel obtained is in the form of an inorganic and amorphous polymer produced by the condensation process of silicate tetrahedrons. The siloxane groups are the interior particles, while the surface is composed of silanol groups (Si–OH). The amorphous silica is also known to have good solubility in solutions of higher than pH 10 (Samantha *et. al.*, 2011; Kalapathy *et al.*, 2000).

In the fabrication process of polymer composite, the prime technique for polymer modification is crosslinking process. In the process, the polymer chain is extended, thus leading to the formation of network structures, which are also seen as a process of stabilisation. The high degree of crosslinking results in better physical properties of the composites (Sherazi, 2015).

A previous study added tetraethyl orthosilicate to thin-film composite membranes to evaluate their mechanical and antifouling capabilities (Norin *et al.*, 2016). In the sol-gel reaction, silica was hydrolysed, and then the hydroxyl groups were condensed to create a nanostructure. The study demonstrated that the membrane's mechanical and antifouling qualities had been enhanced by the inclusion of both glycerol and tetraethyl orthosilicate to the formulation.

Besides reducing the fouling, adding additives such as titanium dioxide, zeolite, and silica is likely to enlarge the macrovoid formation that will improve the interconnectivity of pores, hence leading to increased porosity of the structures of the membranes (Zawati *et al.*, 2013). The membrane properties such as physical properties, mechanical characteristics, and pore distributions can be modified with the incorporation of additives (Taurozzi *et al.*, 2008). An optimal membrane structure due to suppression of macrovoids, antifouling mechanism, increased flux permeation, and higher rejection on membrane performance can be accomplished with a variety of additive concentrations (Jamalludin *et al.*, 2013). Zawati *et al.* have reported that the presence of silica can make the membrane withstand chemical attacks and have high thermal stability. Furthermore, silica owns strong hydrophilic properties that can prevent fouling mechanisms through membrane permeability properties enhancement.

As an effort to substitute the silica with an abundant biomass material, this research was conducted with the aims to study the effect of incorporating the extracted silica from RHA on the crosslinking structure of the produced membranes and their pure water flux respectively, and to evaluate the effectiveness of the modified acid leaching process to extract the silica from RHA.

For the membrane formulation, the silica powder was incorporated into the membrane solution consisting of polyvinyl alcohol and chitosan at a 1:1 weight ratio, which was then further blended with a polysulfone solution. Chitosan was chosen as the raw material because the produced membrane would be later used to remove any heavy metals. After all, chitosan is an excellent biosorbent for heavy metal ions as it contains a large number of amino and hydroxyl groups (Leo *et al.*, 2012). However, to overcome its low mechanical stability and poor chemical resistance, the chitosan was blended with polyvinyl alcohol (PVA) and polysulfone, respectively, to yield a membrane that possessed additional advantages of high hydrophilicity, good physicochemical, mechanical, and hydraulic stability (Leo *et al.*, 2012). Polyethylene glycol was also added together with polysulfone as a pore-forming agent to increase the pore size of the membrane.

II. MATERIALS AND METHOD

A. Materials

The purchases of polyvinyl alcohol with a molecular weight of 85,000–124,000 and 87–89% hydrolysed as well as polysulfone with a molecular weight of 22,000 were made from Sigma-Aldrich (M) Sdn. Bhd., Subang, Malaysia. The chitosan (CS) was procured from Aman Semesta Enterprise in Shah Alam, Malaysia. The polyethylene glycol 400 and 1-methyl-2-pyrrolidone (NMP) were bought from Merck Sdn. Bhd. in Selangor, Malaysia. The dimethyl sulfoxide and

hydrochloric acid (HCl, 37% purity) were bought from R&M Chemicals in Subang, Malaysia. The supplier of the RHA was BT Science Sdn. Bhd. in Selangor, Malaysia. Both deionised (DE) and distilled (DI) water were obtained from UiTM Shah Alam's chemical laboratory in Malaysia.

B. Methods

1. Silica extraction method for rice husk ash

Cleaning the raw material was the first step in the procedure. 250mL of distilled water and 50g of raw RHA was combined, along with 8g of HCl. The mixture was then heated to 90°C and agitated at 650rpm for 1h. After cooling the mixture overnight, it was filtered using a filter paper Smith 102 and left overnight. The RHA was then combined with 250mL of 1M NaOH, heated to 80°C, and agitated for 1h at 600rpm. The mixture was again allowed to cool to room temperature overnight before being filtered through a filter paper (Smith 102). Following a pH measurement, the liquid obtained was reddish and had a pH of 14. The pH was then adjusted to 7 by further HCl (1N) treatment.

The gel was then washed and vigorously stirred at 1,500rpm with 400mL of distilled water. To remove sodium chloride (NaCl) and obtain high purity of silica oxide (SiO2) and water, the washing process was repeated until clear gel was obtained. The gel was dried in an oven at 60°C for 24h. Dried silica gel was obtained and crushed into powder. The properties of the RHA–Silica (RHA–Si) powder were characterised using X-Ray Diffractometer (XRD) and X-Ray Fluorescence (XRF) (Samantha *et al.*, 2011). The process involved in the preparation of silica gel is expressed in Equation (1) and Equation (2) below.

$$(SiO_2)x(s) + 2H_2O(1) \rightarrow (SiO_2)x - 1(s) + Si(OH)4(aq.) \quad (1)$$

$$(Na_2SiO_3) + H_2O + 2HCl \rightarrow Si(OH)4 + 2NaCl \quad (2)$$

2. PVA and CS solutions

PVA solution was made by combining 10g of PVA powder with 90g of dimethyl sulfoxide and heating at 90°C for 4h while being stirred at 400rpm. Meanwhile, the CS solution was made by combining 0.02g of CS powder with 99.98g of aqueous acetic acid (2wt%) and heating at 90°C and stirring at 400rpm for 4h. Both solutions were allowed to cool to room temperature (Sulaiman *et al.*, 2016).

3. Polysulfone solution

Polysulfone solution was made by mixing 13g of polysulfone beads with 82g of NMP and 5g of polyethylene glycol (PEG 400). The mixture was then heated and stirred for 6h at 60°C and 400rpm, respectively. The solution was allowed to cool to room temperature (Kassim Shaari *et al.*, 2019).

4. Hybrid membrane with RHA–Si powder

PVA solution and CS solution were mixed and stirred at 400rpm for 7h with a heating temperature of 60°C. The RHA-Si powder was added at two different concentrations (Liao *et. al.*, 2015; Zawati *et al.*, 2013). Next, 1mL of HCl was added during the sol-gel process as a catalyst. Then, the solution was cooled to room temperature. The above procedures were repeated without the addition of RHA–Si powder as a control membrane (Kassim Shaari *et. al.*, 2019; Sulaiman *et al.*, 2016). Table 1 depicts the details of the formulations prepared in this study.

Table 1. Hybrid membranes formulations

Membrane	PVA solution (g)	CS solution (g)	RHA powder (wt%)	HCl 37% (w/w) (mL)
Mo	50	50	0	1
M1	50	50	0.05	1
M2	50	50	2.5	1

5. Integral membrane

The integral membrane was prepared by adding 1g of Mo solution, as shown in Table 1, to 50g polysulfone solution. The mixture was heated 80°C and stirred at 700rpm for 3h. The same method was repeated for hybrid membrane solutions, M1 and M2 respectively.

C. Chemical Analysis of RHA–Si

The pattern of RHA–Si powder was examined using XRD, specifically the Rigaku XRD, model D/Max 2200V/PC. The

acceleration voltage was set to 40kV, the current to 30mA, and the diffraction angle was set to 2θ with a rate of 5˚ /min (Kalapathy *et al.*, 2000). The element composition in the RHA–Si powder was determined using XRF, specifically the Panalytical Axios, model HP DC7900 (Setyawan *et al.*, 2019).

D. Membrane Analysis

The functional groups of elements in the integral membrane were identified using Fourier Transform Infrared Spectroscopy (FTIR). By generating an infrared absorption spectrum, this analysis identified chemical bonds in the molecule. The model was Perkin Elmer Spectrum 400. The wavelength range of the integral membrane sample was 400cm^{-1} to 4,000cm^{-1} (Shaari *et al.*, 2012).

Scanning Electron Microscopy (SEM) analysis was conducted using Hitachi SU3500 (351716-01) to identify the morphological structure of the membrane. The membranes were initially coated with copper to eliminate or reduce the electric charge that was built on the membranes when it was scanned under a high-energy electron beam. The charging phenomena during the process may result in image distortion, leading to a high charge that decelerated the primary beam and acted as an electron mirror. The accelerating voltage was adjusted to 15kV with a magnification of ×1.5k.

The contact angle analysis was performed using a contact angle instrument, VCA 3000s by using a sessile drop method. For each membrane, 3 drops of water were used, and the average angle was evaluated from the VCA image.

E. Pure Water Flux Analysis

The pure water flux (PWF) analysis was carried out at room temperature using a dead-end mode of filtration rig, as shown in Figure 1. The pressure was controlled by a nitrogen gas cylinder connected to the rig. By applying 6 bars of pressure to the feed solution, the flux of pure water was measured for 60 minutes, with 15-minute intervals for sampling. The membrane sample, which had a circular shape and a cross-sectional area of 1.96 × 10^{-3} m^2, was placed on the sample housing. The volume collected during the filtration process was used to calculate the flux. For each formulation, three runs were performed, and the average reading was calculated. Equations (3) and (4) are the formulae to calculate the permeate flux.

$$J_p = \frac{Q_p}{A\Delta t} \tag{3}$$

$$Q_p = \frac{W_p}{\rho} \tag{4}$$

In the formulae, Jp is the permeate flux (L/m^{2}h), Qp is the permeate volume (L), A is the effective membrane area (m^2), t is the sampling time (h), Wp is the permeate weight (g), and ρ is the permeate density (g/cm^3) (Ahmad *et. al.*, 2012; Mohammadi & Saljoughi, 2009).

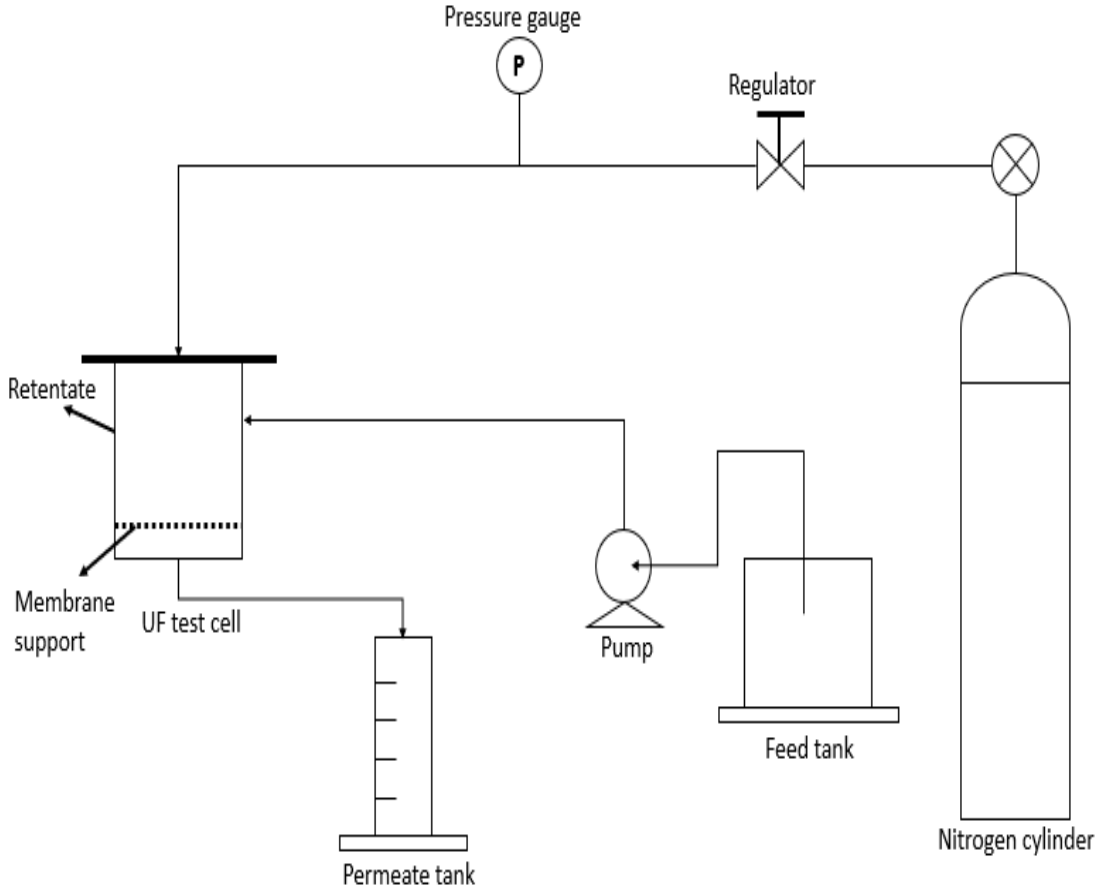

Figure 1. Schematic diagram of the experimental set-up

III. RESULTS AND DISCUSSION

A. Silica Powder Characterisation

Figure 2 shows the pattern of RHA–Si powder samples from the XRD analysis. Figure 2(a) shows the pattern of the extracted silica powder with an insufficient washing process, where the powder still contained NaCl residue. The fingerprints of the residues were evidenced through the peaks that appeared at 32°, 46°, and 57° (Setyawan *et al.*, 2019). As a comparison, Figure 2(b) displays the residue-free image of RHA–Si powder after a complete cycle of the washing process, which portrayed a similar pattern to that obtained by Kalapathy *et al.* (2000), as shown in Figure 2(c). These results showed that the modified extraction process was successfully conducted and managed to achieve a high purity of SiO_2. Overall, both patterns (a) and (b) portrayed that the silica powder obtained was in an amorphous state (Jamalludin *et. al.*, 2013; Geetha *et al.*, 2016). The presence of NaCl residue was because the gel was not thoroughly washed before proceeding to the drying process. With regards to the application of silica powder as a filler in the membrane fabrication, the presence of NaCl in the silica powder could affect the cross-linking properties of the integral membrane (Kalapathy *et. al.*, 2000; Samantha *et al.*, 2011).

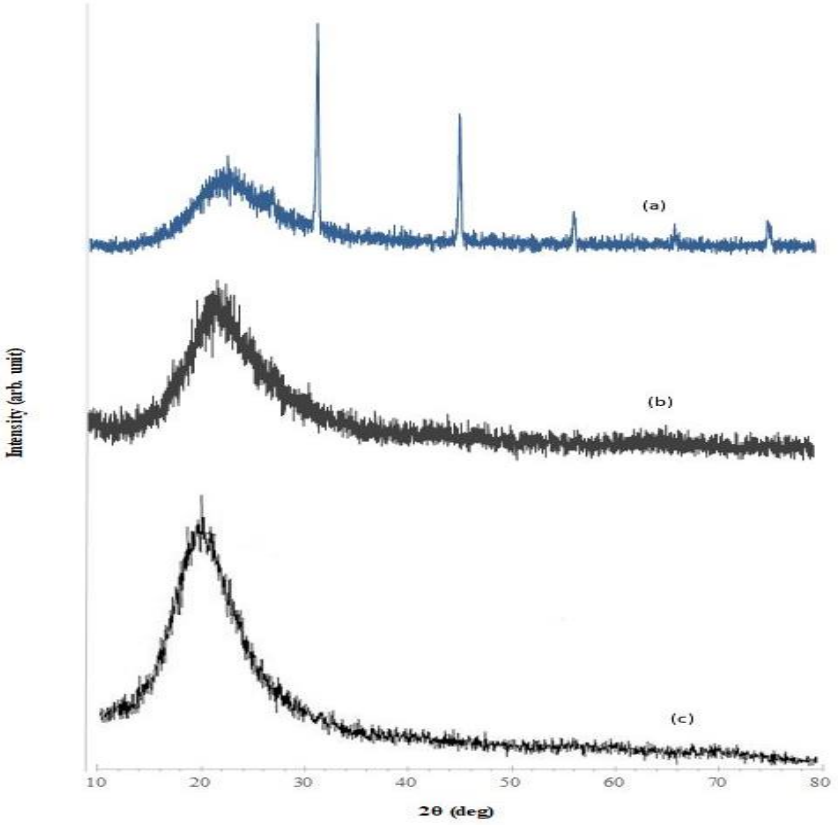

Figure 2. X-ray diffraction data of RHA–Si powder (a) RHA–Si powder with NaCl trace, (b) RHA–Si powder with high purity, and (c) RHA–Si powder from Kalaphaty *et al.* (2000)

Next, the XRF analysis was conducted to analyse the chemical composition of the RHA–Si powder. As shown in Table 2, 77.02% of silica, 0.49% of Na, and 0.53% of Cl were obtained from the extraction process. Meanwhile, another 21.97% was from oxides and metal impurities. Setyawan *et al.* obtained 86.17% of SiO_2, while Kalapathy *et al.* obtained 93%, and the results were higher compared to this research (Setyawan *et. al.*, 2019; Kalapathy *et al.*, 2000). The different sources of RHA used might also possibly be the cause. However, as long as only traces of NaCl were present in the RHA–Si powder, the subsequent crosslinking process of the membrane would not be affected.

Table 2. Chemical element composition of RHA–Si powder

Compound	Percentage (%)
Si	77.02
Na	0.49
Cl	0.53
Others	21.97

Figure 3 depicts the FTIR spectra of RHA–Si powder. The spectra revealed the presence of a few major chemical groups. Silanol –OH groups dominated the vibration band between 2,800cm^{-1} and 3,600cm^{-1} (Kalapathy *et. al.*, 2000; Geetha *et al.*, 2016). The absorption bands were at 1,074cm^{-1} and 790cm^{-1} for Si–O–Si and Si–O, respectively (Ravi & Selvaraj, 2014; Jean *et. al.*, 2011; Alias *et al.*, 2020).

The bending vibration band at 470cm^{-1} was associated with O–Si–O bond (Joni *et al.*, 2018). Small bending and stretching vibration band of Si–OH were situated at a peak of 960cm^{-1} (Feifel & Lisdat, 2011).

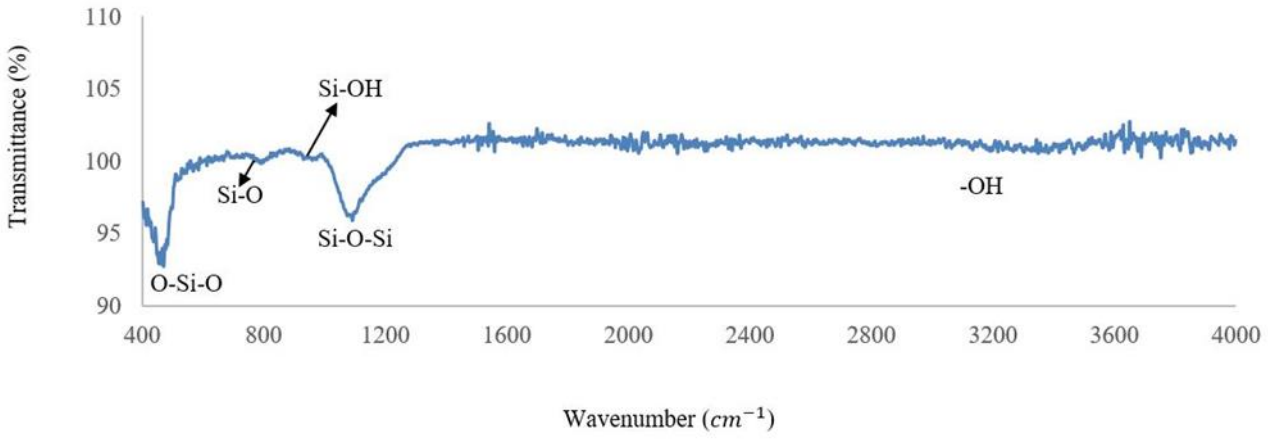

Figure 3. FTIR analysis for RHA–Si powder

Figure 4 displays the image of RHA–Si powder from SEM analysis. It was observed that the RHA–Si powder contained various sizes with the main size was around 150µm.

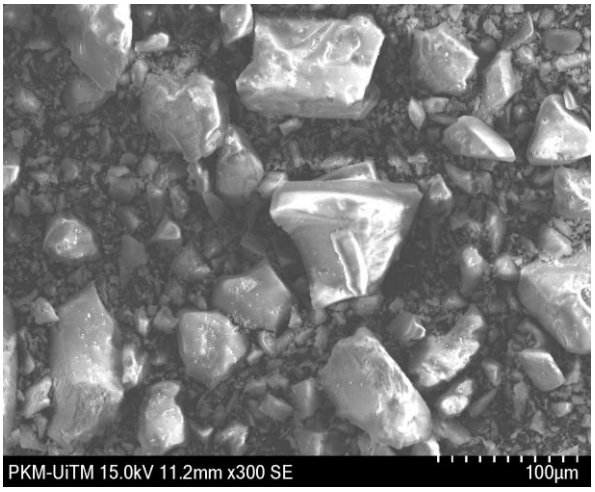

Figure 4. SEM analysis for RHA–Si powder

B. Membrane Characterisation

Figures 5(a), (b), and (c) demonstrate the FTIR spectra for M0, M1, and M2, respectively. Overall, the pattern of the spectra for M0 and membranes with silica powder (M1 and M2) showed a major difference at a range of 1,600cm^{-1} to 4,000cm^{-1}, as shown in Figures 5(b) and 5(c). On the other hand, as shown in Figure 5(a), the absorption band in the range of 1,000cm^{-1} to 1,100cm^{-1} corresponded to the Si–O stretching band (Ruan *et al.*, 2010). The 1,100cm^{-1} to 1,700cm^{-1} peaks were caused by the vibration modes of C=O and C–O bonds in unhydrolysed vinyl acetate from PVA (Shaari *et al.*, 2012). The spectra absorption of Si–C and Si–O bonds reacted with the original C–O bond to form Si–O–C at the peak 1,105 cm^{-1} for membranes M1 and M2, demonstrating the successful occurrence of the crosslinking reaction using the RHA–Si powder (Oh & Choi, 2010). As shown in Figure 5(c), in the range of 2,800cm^{-1} to 3,900cm^{-1}, M1 and M2 had lower stretching bands compared to M0 due to the presence of silanol groups from RHA–Si powder and hydroxyl groups (–OH) from PVA. The small peaks present at 3,783cm^{-1} and 3,675cm^{-1} showed the presence of –OH groups in the membrane. The presence of –OH groups stretching in all membranes showed that the hydrophilicity of the membrane was enhanced regardless of the crosslinking process that occurred, which would then improve the performance of the membrane (Alias *et al.*, 2020).

Another peak assigned as the hydroxyl group is at 1,600cm^{-1}. The strong bands in M2 at 2,327cm^{-1} and 2,115cm^{-1} might be due to O=C=O stretching and the absorption band of C≡C, respectively as shown in Figure 5(b) (Asep *et al.*, 2019). An asymmetric stretching of the C–H bond was found at peaks 2,851cm^{-1} and 2,922cm^{-1} in M0 as shown in Figure 5(c), as well as the peaks around 2,970cm^{-1} for all membranes, thus indicating C–H bond stretching (Asep *et al.*, 2019). All membranes had C–H stretching that coincided with amine bands at the peaks between 2,800cm^{-1} and 3,000cm^{-1} (Sulaiman *et al.*, 2016).

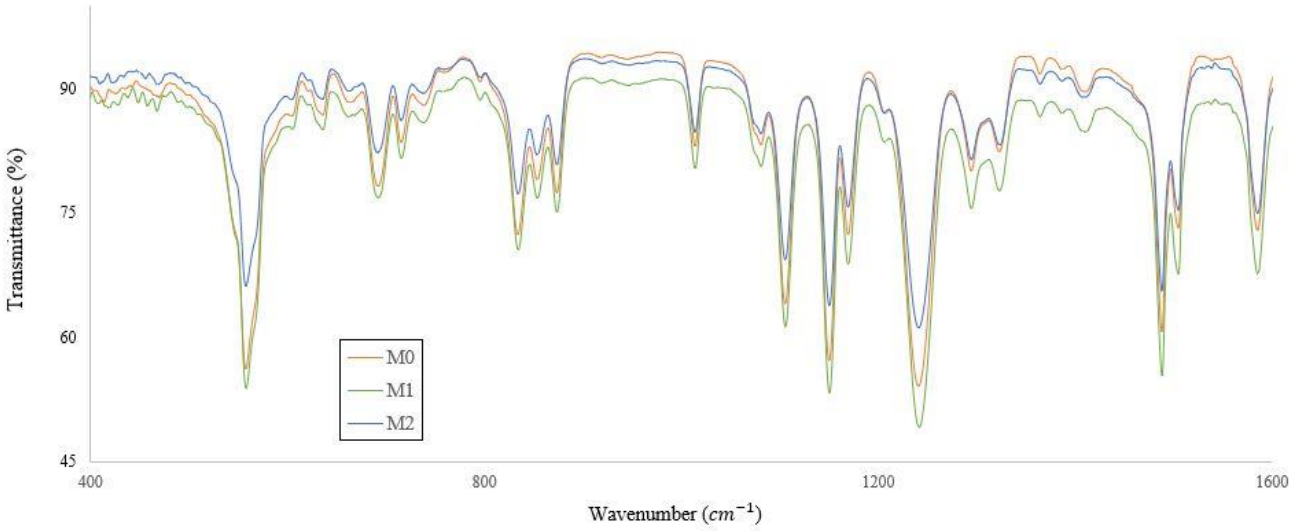

Figure 5(a). FTIR analysis ranging from 400cm⁻¹ to 1,600cm⁻¹

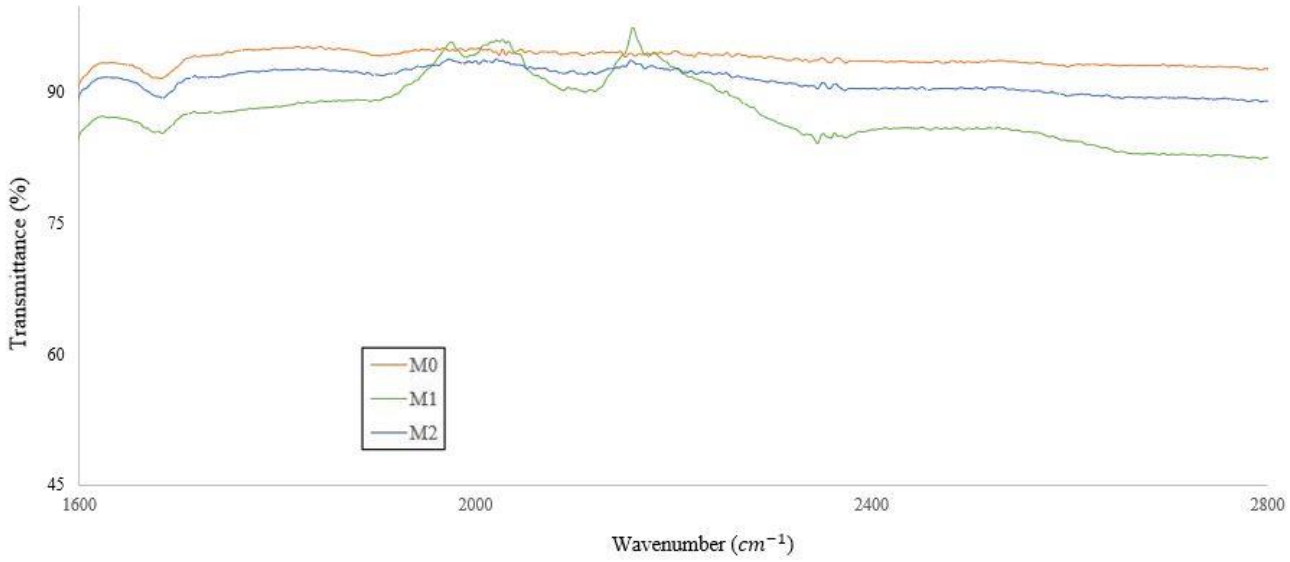

Figure 5(b). FTIR analysis ranging from 1,600cm⁻¹ to 2,800cm⁻¹

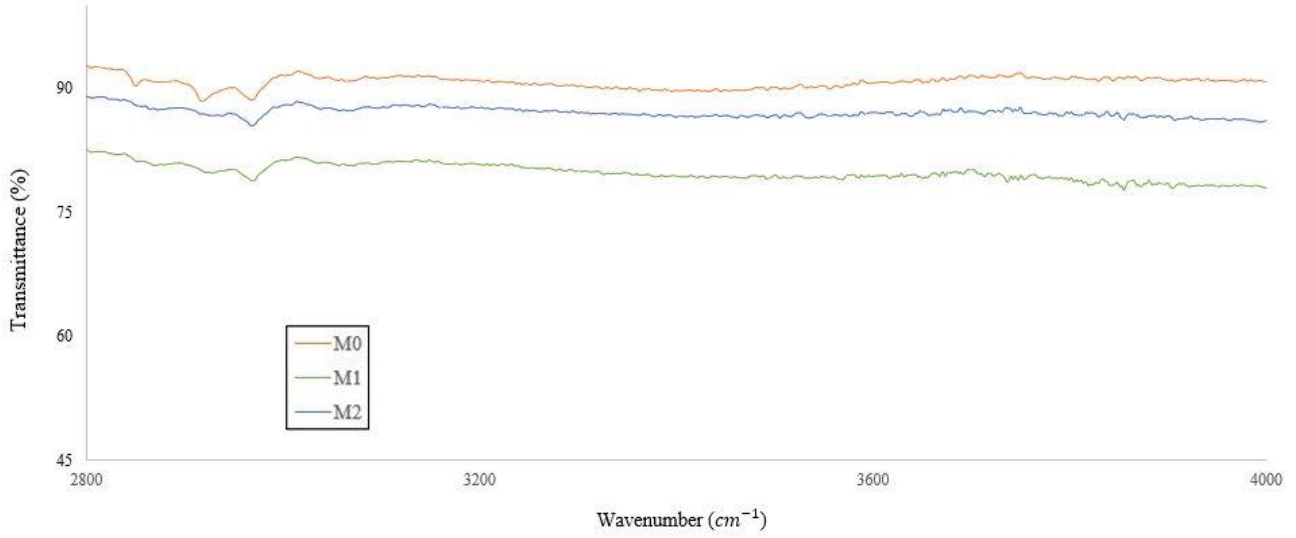

Figure 5(c). FTIR analysis ranging from 2,800cm⁻¹ to 4,000cm⁻¹

The surface morphology of all membranes is depicted in Figure 6. As shown in the figure, a more compact structure was observed with the incorporation of silica powder in the membrane M1 and M2 as compared to M0. The dense structure of membranes as a result of crosslinking process between the hydroxyl group from the polymer with Si–O–H from the silica powder provides more adsorption area, which is highly preferred when the membrane is to be used for heavy metal ion removal (Shaari *et al.*, 2012). Based on the surface structure of the membranes and the average pore sizes, it showed the membranes had homogenous structures, which suggested that the crosslinking process with the RHA–Si powder was complete (Ye *et al.*, 2007).

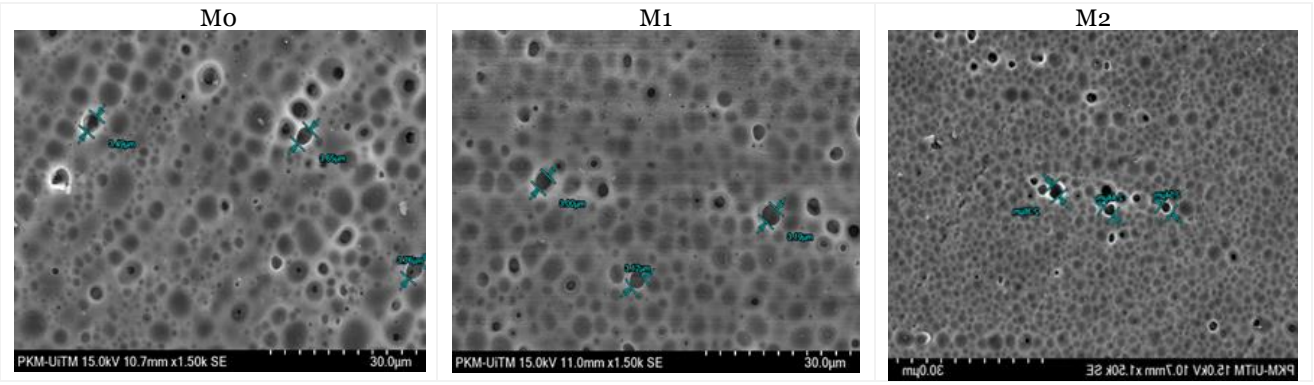

Figure 6. SEM images of M0, M1, and M2

Next, contact angle analysis was performed to evaluate the surface hydrophilicity or hydrophobicity of the membranes, where a high value corresponds to the hydrophobicity of the membrane's surface (Shi *et al.*, 2013). As shown in Figure 7, the incorporation of RHA–Si powder resulted in the increased hydrophobicity of the membrane's surface. The contact angle of the membrane for M1 and M2 also increased as the concentration of RHA–Si powder increased. This was because the value increased from 78.9° to 91.2°. The result also indicated that M2 was more hydrophobic than M1 and M0 (Gohil & Ray, 2009).

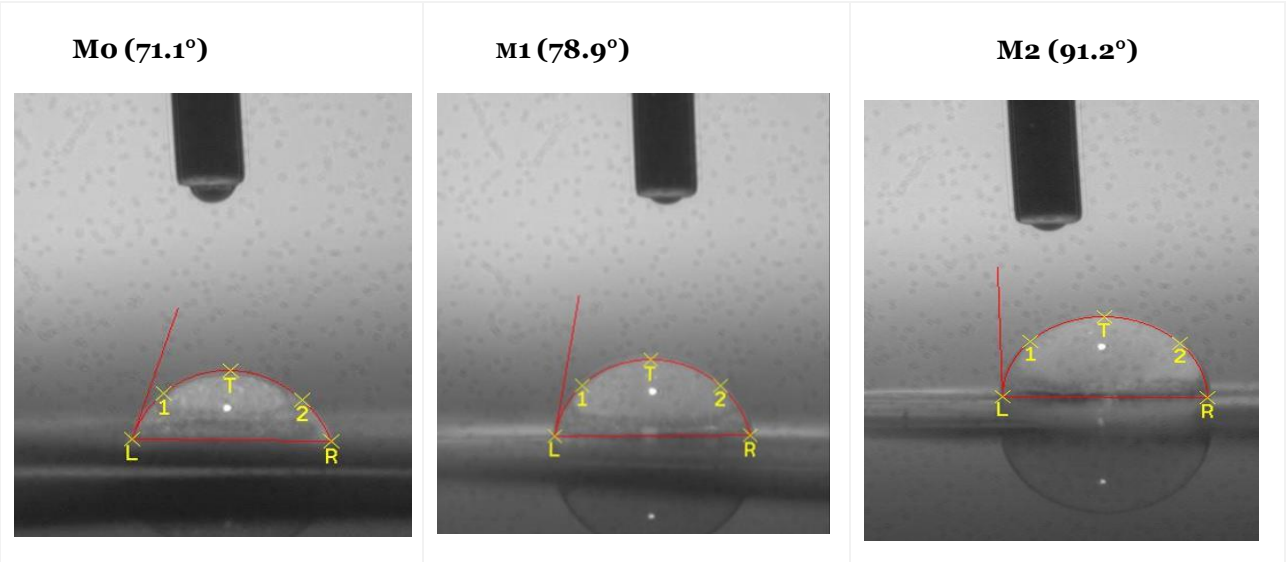

Figure 7. Contact angle images of M0, M1, and M2

Figure 8 shows the XRD images of membranes with different percentages of RHA–Si powder. As shown in the figure, for M1 and M2, their peak intensity dampened proportionally with the increment of RHA–Si powder

incorporated in the membrane's formulation. This result confirms that the incorporation of RHA–Si powder at various percentages was successful to yield an amorphous structure of membrane (Ali *et. al.*, 2021; Jamalludin *et al.*, 2013). The amorphous structures were obtained due to the crosslinking process, which was preferred as the brittle structure of the membrane could be reduced (Alqaheem & Alomair, 2020; Asran *et al.*, 2010).

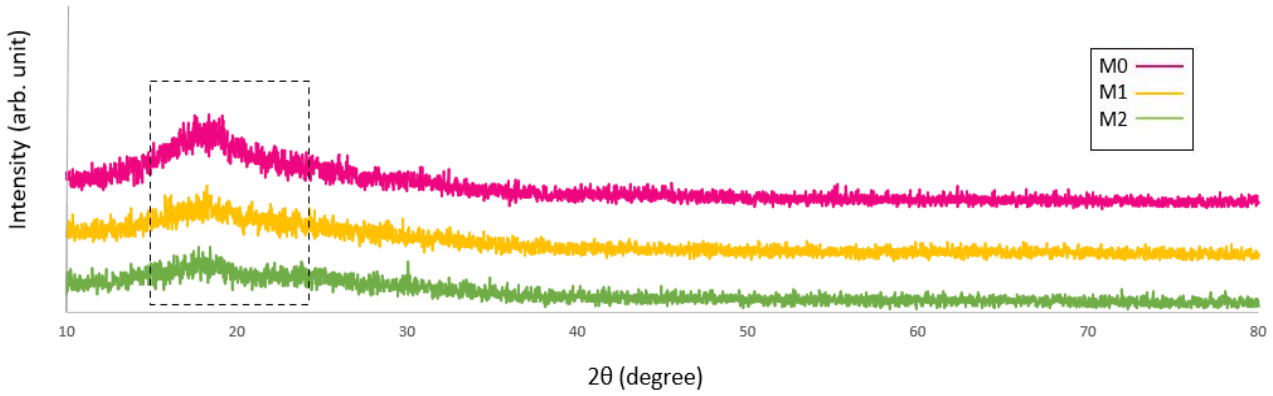

Figure 8. XRD images of membranes (M0, M1, and M2)

C. Pure Water Flux Performance

Figure 9 shows the flux of M0, M1, and M2 in the 1-hour filtration process. Pure water flux (PWF) results portray the surface membrane hydrophilicity and its pore size (Ahmad *et al.*, 2012), where the pure water permeability is displayed through the porous structure of the membrane (Košutić *et al.*, 2006). Pure water permeability should be linear with the pressure if the membrane porosity remains the same. However, if the water flux is not constant, there are changes in the membrane structure (Košutić *et al.*, 2006).

The above situation was portrayed by M0, where the flux kept increasing until 1h, showing that the water permeation of the membrane increased because the changes in pore sizes of the membrane occurred (Tian *et al.*, 2017). This condition was due to the lack of structural stability since there was no silica present in the membrane, and the PVA contained a high amount of hydroxyl groups. Thus, the swelling behaviour of the membrane was expected (Danielli *et al.*, 2020).

For the M1, the flux showed a different trend. During the first 15 mins of filtration, the flux decreased due to concentration polarisation because of a build-up layer of the adsorbed ions. However, the trend showed a consistent value until 1h of filtration time. The M1 with a 78.9° contact angle still showed a hydrophilic property of the membrane, where the presence of RHA–Si powder at 0.05wt% enhanced the stability of the mechanical membrane structure throughout the filtration process. This condition showed that the crosslinking reaction did not only make the membrane denser but also offered a great stability to it (Danielli *et al.*, 2020). A much lower flux portrayed by M2 could be related to its denser surface, as depicted in Figure 6, due to the high loading of RHA–Si powder that resulted in M2 having a hydrophobic property.

Even though the crosslinking reaction suppressed the hydroxyl group of polymer blend, the hydrophilic character of silica compensated the effect where M1 still allowed for a high permeation of water and a consistent value of flux (Xu *et. al.*, 2015; Alias *et al.*, 2020).

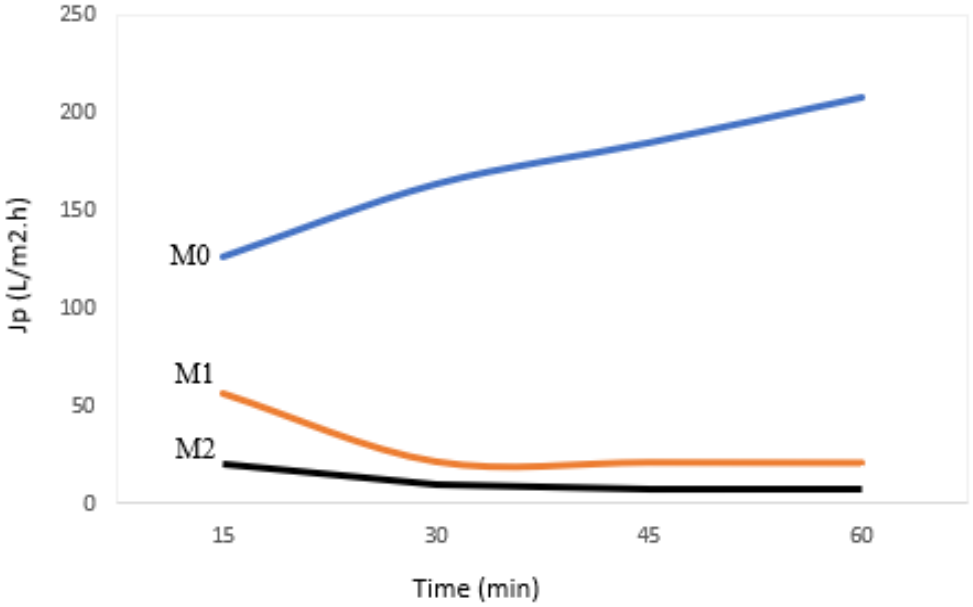

Figure 9. Pure water flux performance analysis

IV. CONCLUSION

To conclude, the extraction of silica from RHA using the modified extraction process was successfully performed as the process managed to remove NaCl and achieved high purity of silica powder with 77.02%. The RHA–Si powder was also compatible with the membrane solution as no separate layer was formed. The results from SEM and FTIR analysis respectively proved the crosslinked structure of the hybrid membranes (M1 and M2). Pure water flux analysis proved that the membranes (M1 and M2) incorporated with RHA–Si powder had better integral stability compared to the membrane from a pure polymer blend (M0). M1 had better properties in terms of pure water flux and surface structure. With this promising result, the test on the actual wastewater containing natural organic matter will be executed in the future to further examine the antifouling behaviour of the membrane, which will be subsequently used to treat the wastewater containing heavy metal ions. Furthermore, the use of RHA in the membrane fabrication does not only reduce the waste generated but also provide value addition to biomass.

V. ACKNOWLEDGEMENT

The research was funded by Universiti Teknologi MARA (UiTM) with a grant file number 600-RMC/GPK 5/3 (119/2020). The authors would like to thank the College of Engineering, UiTM Shah Alam for the publication sponsorship.

VI. REFERENCES

Ahmad, AL, Yusuf, NM & Seng, O 2012, 'Preparation and Modification of Poly (vinyl) Alcohol Membrane: Effect of Crosslinking Time Towards Its Morphology', Desalination, vol. 287, pp. 35–40.

Ali, AM, Rashid, KT, Yahya, AA, Majdi, HS, Salih, IK, Yusoh, K, Alsalhy, QF, Abdulrazak, AA & Figoli, A 2021, 'Fabrication of Gum Arabic-Graphene (GGA) Modified Polyphenylsulfone (PPSU) Mixed Matrix Membranes: A Systematic Evaluation Study for Ultrafiltration (UF) Applications', Membranes, vol. 11, p. 542.

Alias, SS, Harun, Z, Manoh, N & Jamalludin, MR 2020, 'Effects of Temperature on Rice Husk Silica Ash Additive for Fouling Mitigation by Polysulfone–RHS Ash Mixed-Matrix Composite Membranes', Polymer Bulletin, vol. 77, pp. 4043-4075.

Alqaheem, Y & Alomair, AA 2020, 'Microscopy and Spectroscopy Techniques for Characterization of Polymeric Membranes', Membranes, vol. 10, p. 33.

Asep, BDN, Rosi, O & Risti, R 2019, 'How to Read and Interpret FTIR Spectroscope of Organic Material', Indonesian Journal of Science & Technology, vol. 4, pp. 97-118.

Asran, AS, Henning, S & Michler, GH 2010, 'Polyvinyl Alcohol–Collagen–Hydroxyapatite Biocomposite Nanofibrous Scaffold: Mimicking the Key Features of Natural Bone at the Nanoscale Level', Polymer, vol. 51, pp. 868-876.

Danielli, AROdS, Luana, CZ & Agnes, dPS 2020, 'Preparation and Characterization of a Novel Green Silica/PVA Membrane for Water Desalination by Pervaporation', Separation and Purification Technology, vol. 247, p. 116852.

Edson Lf, RH, Rejane SH, Utingguassu LP & Sergio LJ 2005, 'Applicability of Rice Husk Ash', Quimica Nova, vol. 28, pp. 1055-1060.

Feifel, S & Lisdat, F 2011, 'Silica Nanoparticles for the Layer-by-layer Assembly of Fully Electro-active Cytochrome C Multilayers', Journal of Nanobiotechnology, vol. 9, p. 59.

Geetha, D, Ananthiand, A & Ramesh, PS 2016, 'Preparation and Characterization of Silica Material from Rice Husk Ash An Economically Viable Method', Journal of Pure and Applied Science, vol. 4, pp. 20-26.

Gohil, JM & Ray, P 2009, 'Polyvinyl Alcohol as the Barrier Layer in Thin Film Composite Nanofiltration Membranes: Preparation, Characterization, and Performance Evaluation', Journal of Colloid and Interface Science, vol. 338, pp. 121-127.

Jamalludin, MR, Harun, Z, Basri, H, Yunos, MZ & Shohur, MF 2013, 'Performance Studies of Polysulfone-Based Membrane: Effect of Silica Morphology', Applied Mechanics and Materials, vol. 372, pp. 8-12.

Jean, SC, Renan, CFL, Nagila, MPSR, Judith, PAF, Edvani, CM & Francisco, HAR 2011, 'Hydrogels Composite of Poly(acrylamide-co-acrylate) and Rice Husk Ash. I. Synthesis and Characterization', Journal of Applied Polymer Science, vol. 123, pp. 879-887.

Joni, IM, Nulhakim, L, Vanitha, M & Panatarani, C, 'Characteristics of Crystalline Silica (SiO2) Particles Prepared by Simple Solution Method Using Sodium Silicate (Na2SiO3) Precursor', J. Phys. Conf. Ser., 2018/08 2018, IOP Publishing, 012006.

Kalapathy, U, Proctor, A & Shultz, J 2000, 'A Simple Method for Production of Pure Silica from Rice Hull Ash', Bioresource Technology, vol. 73, pp. 257-262.

Kassim Shaari, NZ, Sulaiman, NA & Rahman, NA 2019, 'Thin Film Composite Membranes: Preparation, Characterization, and Application Towards Copper Ion Removal', Journal of Environmental Chemical Engineering, vol. 7, p. 102845.

Košutić, K, Dolar, D & Kunst, B 2006, 'On Experimental Parameters Characterizing the Reverse Osmosis and Nanofiltration Membranes' Active Layer', Journal of Membrane Science, vol. 282, pp. 109-114.

Leo, CP, Cathie Lee, WP, Ahmad, AL & Mohammad, AW 2012, 'Polysulfone Membranes Blended with ZnO Nanoparticles for Reducing Fouling by Oleic Acid', Separation and Purification Technology, vol. 89, pp. 51-56.

Liao, G, Yang, C, Hu, C, Pai, Y & Lue, S 2015, 'Novel Quaternized Polyvinyl Alcohol/Quaternized Chitosan Nano-composite as an Effective Hydroxide-Conducting Electrolyte', Journal of Membrane Science, vol. 485, pp. 17-29.

Mohammadi, T & Saljoughi, E 2009, 'Effect of Production Conditions on Morphology and Permeability of Asymmetric Cellulose Acetate Membranes', Desalination, vol. 243, pp. 1-7.

Norin, ZKS, Norazah, AR, Nurul, AS & Ramlah, T, 'Thin Film Composite Membranes: Mechanical and Antifouling Properties', MATEC Web Conf., 01/01 2016, EDP Sciences, 06005.

Oh, T & Choi, CK 2010, 'Comparison Between SiOC Thin Films Fabricated by Using Plasma Enhance Chemical Vapor Deposition and SiO2 Thin Films by Using Fourier Transform Infrared Spectroscopy', Journal of the Korean Physical Society, vol. 56, pp. 1150-1155.

Rasoul, BI, Günzel, FK & Rafiq, MI 2018, 'Effect of Rice Husk Ash Properties on the Early Age and Long Term Strength of Mortar', in: Hordijk, D & Luković, M (eds.) High Tech Concrete: Where Technology and Engineering Meet. Netherlands: Springer.

Ravi, S & Selvaraj, M 2014, 'Incessant Formation of Chain-Like Mesoporous Silica with a Superior Binding Capacity for Mercury. Dalton Transactions', vol. 43, pp. 5299-5308.

Ruan, D-S, Li, Y-L, Wang, L, Su, D & Hou, F 2010, 'Fabrication of Silicon Oxycarbide Fibers From Alkoxide Solutions Along the Sol–Gel Process', Journal of Sol-Gel Science and Technology, vol. 56, pp. 184-190.

Samantha, PBL, Raimundo, PVO, Guilherme, CC, Marcia, RMC & Romildo, DTF 2011, 'Production of Silica Gel from Residual Rice Husk Ash Química Nova', vol. 34, pp. 71-75.

Setyawan, N, Hoerudin & Wulanawati, A 2019, 'Simple Extraction of Silica Nanoparticles from Rice Husk Using Technical Grade Solvent: Effect of Volume and Concentration', IOP Conference Series: Earth and Environmental Science, vol. 309, p. 012032.

Shaari, NZK, Rahman, NA & Tajuddin, RM 2012, 'Thin Film Composite Membrane With Hybrid Membrane as the Barrier Layer: Preparation and Characterization', 2012 IEEE (CHUSER), 3-4 Dec. 2012, IEEE Colloquium on Humanities, Science and Engineering (CHUSER), IEEE Xplore, pp. 615-620.

Sherazi, T 2015, 'Graft Polymerization', in: Enrico, D & Lidietta, G (eds.) Encyclopedia of Membranes, Berlin: Springer Berlin Heidelberg.

Shi, F, Ma, Y, Ma, J, Wang, P & Sun, W 2013, 'Preparation and Characterization of PVDF/TiO2 Hybrid Membranes with Ionic Liquid Modified Nano-TiO2 Particles', Journal of Membrane Science, vol. 427, pp. 259-269.

Sldozian, R 2014, 'Comparison Between the Properties of Amorphous and Crystalline - Nano SiO2 Additives on Concrete', IJSE, vol. 5, pp. 1437–1443.

Sulaiman, NA, Shaari, NZK & Rahman, NA 2016, 'Removal of CU (II) and FE (II) Ions Through Thin Film Composite (TFC) with Hybrid Membrane', Journal of Engineering Science and Technology, vol. 11, pp. 36-49.

Taurozzi, JS, Arul, H, Bosak, VZ, Burban, AF, Voice, TC, Bruening, ML & Tarabara, VV 2008, 'Effect of Filler Incorporation Route on the Properties of Polysulfone–Silver Nanocomposite Membranes of Different Porosities', Journal of Membrane Science, vol. 325, pp. 58-68.

Tian, S, Ren, W, Li, G, Yang, R & Wang, T 2017, 'A Theoretical Analysis of Pore Size Distribution Effects on Shale Apparent Permeability', Geofluids, 7492328.

Xu, H-P, Yu, Y-H, Lang, W-Z, Yan, X & Guo, Y-J 2015, 'Hydrophilic Modification of Polyvinyl Chloride Hollow Fiber Membranes by Silica with a Weak In Situ Sol–gel Method', RSC Advances, vol. 5, pp. 13733-13742.

Ye, LY, Liu, QL, Zhang, QG, Zhu, AM & Zhou, GB 2007, 'Pervaporation Characteristics and Structure of Poly(vinylalcohol) /Poly(ethylene glycol)/ Tetraethoxysilane Hybrid Membranes', Journal of Applied Polymer Science, vol. 105, pp. 3640-3648.

You, PY, Kamarudin, SK & Masdar, MS 2019, 'Improved Performance of Sulfonated Polyimide Composite Membranes with Rice Husk Ash as a Bio-filler for Application in Direct Methanol Fuel Cells', International Journal of Hydrogen Energy, vol. 44, pp. 1857-1866.

Zawati, H, Mohd, RJ, Hatijah, B, Muhammad, FS, Nurafiqah, R & Muhamad, ZY 2013, 'The Effect of Synthetic Silica on Ultrafiltration PSf Membrane', Jurnal Teknologi, vol. 65, pp. 121-125.